COHERENCE BOUNDS FOR SENSING MATRICES IN SPHERICAL HARMONICS EXPANSION

Arya Bangun, Arash Behboodi and Rudolf Mathar

Institute for Theoretical Information Technology
RWTH Aachen University, D-52074 Aachen, Germany
Email: {bangun,behboodi,mathar}@ti.rwth-aachen.de

ABSTRACT

The mutual coherence provides a basis for deriving recovery guarantees in compressed sensing. In this paper, the mutual coherence of spherical harmonics sensing matrices is examined for a class of sensing patterns common in practice and is used as a figure of merit for designing sensing matrices. We will show that for each sampling pattern, the coherence is lower bounded by the inner product of two Legendre polynomials with different degrees. In some practical situation, it is desirable to have sampling points on a sphere follow a regular pattern, hence, facilitating the measurement process. It will be shown that for a class of sampling patterns, the mutual coherence would be at its maximum, yielding the worst performance. Finally, the sampling strategy is proposed to achieve the derived lower bound.

Index Terms— Coherence, sparse recovery, spherical harmonics

1. INTRODUCTION

In compressed sensing, there are well known conditions on the sensing matrix for stable and robust signal recovery. The Restricted Isometry Property (RIP) provides recovery guarantees for sparse signal and it has been proven that random matrices with sub-Gaussian distribution satisfy RIP with high probability. Unlike RIP [1, 2], the mutual coherence can be numerically evaluated for a given matrix and therefore it is a computable figure of merit for sparse recovery. For a matrix $\mathbf{A} = (\mathbf{a}_1, \mathbf{a}_2, \ldots, \mathbf{a}_N) \in \mathbb{C}^{m\times N}$, the mutual coherence of $\mathbf{A}$ is defined as

$$\mu(\mathbf{A}) = \max_{1\leq q\neq r\leq N} \frac{|\langle \mathbf{a}_q, \mathbf{a}_r\rangle|}{\|\mathbf{a}_q\|_2 \|\mathbf{a}_r\|_2}. \quad (1)$$

In general, the mutual coherence leads to pessimistic recovery guarantees, usually necessitating very low mutual coherence for comparable recovery guarantees to RIP. The coherence might nonetheless be used for designing deterministic sensing matrices. Particularly in the context of bounded orthonormal systems, the sensing matrix has already some additional structures coming from the orthogonal basis which prevents us from using proposals like those inspired by coding theory [3] for deterministic sensing matrices. Using mutual coherence for design and analysis of deterministic sensing matrices was studied in many different areas, from coding theory [4, 5], communication [6, 7], quantum measurement [8, 9] and machine learning [10, 11]. Specifically in compressed sensing, for example, in [12] the authors define an algorithm to optimize measurement matrix for compressed sensing. The initial idea is to define t-averaged mutual coherence as a threshold and optimize the Gram matrix based on singular value decomposition. Recently, in [13], rather than optimizing the off-diagonal matrix of Gram matrix, the authors try to find a new frame with low mutual coherence property. The same condition applies in [14, Chapter 14], where the authors discuss recovery condition based on the mutual coherence with random signal models, specifically Bernoulli and uniform distribution. In general, sensing matrices with lower mutual coherence provide better sparse recovery guarantees. The mutual coherence is lower bounded by the so called Welch bound, defined in the context of correlation measurements of different signals [15], given as

$$\mu(\mathbf{A}) \geq \sqrt{\frac{N-m}{m(N-1)}}. \quad (2)$$

The bound is achieved, for instance, by considering the Grassmannian frame, which is equiangular and tight [6]. However, it has been shown that this class of frames only exists for certain pairs of m and N [16]. It is moreover difficult or sometimes not possible to find these frames for certain structured matrices, as in bounded orthonormal systems.

In this work, we are interested in coherence-based analysis of sensing matrices that are constructed from spherical harmonics expansion. Spherical harmonics as orthonormal basis are widely used in order to analyze the signal on the sphere, for example, spherical near-field antenna measurement [17], earth magnetic fields [18] and spherical microphone array [19]. In [20, 21], random sensing matrices were discussed for spherical harmonics. Since spherical harmonics are not uniformly bounded, random sensing matrices could only fulfill RIP after appropriate pre-conditioning techniques. Nevertheless, it is desirable to generate sensing matrices with more regular structures in practical applications. For instance, the measurements in antenna design are done using a robotic probe, favoring more smooth and regular movements rather than random movements on the sphere. This paper is organized as follows. In section 2, the main definitions and the properties of spherical harmonics are provided. In section 3, the coherence analysis is conducted for a class of sampling patterns and a lower bound on the coherence itself is derived. Numerical experiments of sparse recovery and computation time of the algorithm to achieve the lower bound are presented in section 4. Finally, the conclusion and future works are discussed in section 5.

1.1. Notation

The elevation and azimuth are denoted by θ and ϕ, respectively. Vectors are presented by small bold letters and matrices by capital bold letters. The set $\{1, ..., m\}$ is denoted by $[m]$.

This work has been funded by DFG project -CoSSTra-MA1184|31-1

2. DEFINITIONS AND BACKGROUNDS

Definition 1 (Spherical harmonics)**.** Spherical harmonics of degree l and order k are defined as follows:

$$\mathrm{Y}_l^k(\theta,\phi) = N_l^k P_l^k(\cos\theta) e^{jk\phi} \tag{3}$$

where $N_l^k = \sqrt{\frac{2l+1}{4\pi}\frac{(l-k)!}{(l+k)!}}$ is the normalization factor and $P_l^k(\cos\theta)$ is the associated Legendre polynomial. For $k=0$, the associated Legendre polynomials become Legendre polynomials $P_l(\cos\theta)$.

Legendre polynomials are either even or odd determined by the relation

$$P_l(-\cos\theta) = (-1)^l P_l(\cos\theta). \tag{4}$$

For $\theta = 0$, it is well known that $P_l(1) = 1$. Furthermore, the Legendre polynomials at 0 are evaluated as

$$P_l(0) = \begin{cases} (-1)^{l/2}\frac{l!}{2^l(\frac{l}{2})!^2} & \text{if } l \text{ is even including } 0, \\ 0 & l \text{ is odd.} \end{cases} \tag{5}$$

Spherical harmonics create a basis for square integrable functions over S^2, that is each function $f \in L^2(\mathrm{S}^2)$ can be written in terms of spherical harmonics as

$$f(\theta,\phi) = \sum_{l=0}^{\infty}\sum_{k=-l}^{l} \hat{f}_l^k\, \mathrm{Y}_l^k(\theta,\phi). \tag{6}$$

This is also called the S^2-Fourier expansion with Fourier coefficient $\hat{f}_l^k$ where

$$\hat{f}_l^k = \int_0^{2\pi}\int_0^{\pi} f(\theta,\phi)\,\overline{\mathrm{Y}_l^k(\theta,\phi)}\sin\theta \mathrm{d}\theta\mathrm{d}\phi. \tag{7}$$

Spherical harmonics are orthonormal with respect to the uniform measure on the sphere $\mathrm{d}\nu = \sin\theta\mathrm{d}\theta\mathrm{d}\phi$, namely:

$$\int_0^{2\pi}\int_0^{\pi} \mathrm{Y}_l^k(\theta,\phi)\overline{\mathrm{Y}_{l'}^{k'}(\theta,\phi)}\sin\theta\mathrm{d}\theta\mathrm{d}\phi = \delta_{ll'}\delta_{kk'} \tag{8}$$

where $\delta_{ll'}$ is Kronecker delta In this work, instead of infinite expansion, we suppose that the functions are bandlimited.

Definition 2 (Bandlimited functions and sparse expansion)**.** A function $f \in L^2(\mathrm{S}^2)$ is bandlimited with bandwidth B if it is expressed in terms of spherical harmonics of degree less than B. A bandlimited function is said to be $s-$sparse if the vector of spherical harmonics coefficients, $\mathbf{f} = (\hat{f}_l^{k,n})$ for $0 \le l \le B-1, -l \le k \le l$, is s-sparse, that is $\|\mathbf{f}\|_0 \le s$.

The sensing matrix $\mathbf{A}$ is constructed using following entries

$$\mathrm{A}_{p,q} = \mathrm{Y}_{l^{(q)}}^{k^{(q)}}(\theta_p,\phi_p), \tag{9}$$

where $p \in [m]$ is the index of a sampling point and $q \in [N]$ is an index used to provide the degree and order of each basis, $l^{(q)}, k^{(q)}$, belonging to the set $\mathcal{J}_\mathcal{S}$:

$$\mathcal{J}_\mathcal{S} = \{(l,k)\,|\,0 \le l \le B-1, -l \le k \le l\} \tag{10}$$

where $|\mathcal{J}_\mathcal{S}| = N = B^2$. It can be seen that the set $\mathcal{J}_\mathcal{S}$ contains combinations between permissible degrees and orders, each pair corresponding to a column. Let the matrix $\mathbf{A} \in \mathbb{C}^{m\times N}$ be constructed from m samples of normalized spherical harmonics, $(\theta_p,\phi_p), p \in [m]$. The mutual coherence of a matrix from spherical harmonics can be written as follow:

$$\mu(\mathbf{A}) = \max_{q\neq r}\left|\sum_{p=1}^{m}\frac{\mathrm{Y}_{l^{(q)}}^{k^{(q)}}(\theta_p,\phi_p)\overline{\mathrm{Y}_{l^{(r)}}^{k^{(r)}}(\theta_p,\phi_p)}}{\|\mathrm{Y}_{l^{(q)}}^{k^{(q)}}(\theta,\phi)\|_2\|\mathrm{Y}_{l^{(r)}}^{k^{(r)}}(\theta,\phi)\|_2}\right| \tag{11}$$

2.1. Spherical near-field antenna measurement

The main application of spherical harmonics and their extension, Wigner-D functions, is the spherical near-field antenna measurement. This is defined in [17] by using the transmission formula as follows:

$$y(\theta,\phi,\chi) = v\sum_{n=-v_{max}}^{v_{max}}\sum_{h=1}^{2}\sum_{l=1}^{B}\sum_{k=-l}^{l} T_{hlk}\mathrm{D}_l^{k,n}(\theta,\phi,\chi) \tag{12}$$

where $y(\theta,\phi,\chi)$ is a bandlimited near-field sample with Wigner-D functions as a basis, h denotes the both transverse electric (TE) and magnetic (TM), n and χ denote order and angle to measure polarization, respectively.

$$\mathrm{D}_l^{k,n}(\theta,\phi,\chi) = N_l e^{-jk\phi}\mathrm{d}_l^{k,n}(\cos\theta)e^{-jn\chi} \tag{13}$$

where $\mathrm{d}_l^{k,n}(\cos\theta)$ is Wigner-d functions. Normally, it is enough to consider co-polarization of the antenna i.e $n = 0$. In this setting, the Wigner-D functions become spherical harmonics, with the following relation

$$\mathrm{D}_l^{-k,0}(\theta,\phi,0) = (-1)^k\sqrt{\frac{4\pi}{2l+1}}\mathrm{Y}_l^k(\theta,\phi). \tag{14}$$

The classical method requires equiangular sampling pattern and uses discrete Fourier transform to estimate the transmission coefficient T_{hlk}. It has been shown already in [22, 23, 24] that, the measurement speed and accuracy in spherical near-field measurement could be improved by using compressed sensing. However, the analysis on deterministic sampling is not yet addressed and we try to address this issue. In particular, it is shown why the equiangular sampling is not proper sampling in term of sparse recovery in spherical harmonics expansion.

3. MAIN RESULT

In order to design a sensing matrix from spherical harmonics, the goal is to find pairs (θ_p,ϕ_p), $p \in [m]$, that minimize the mutual coherence of the sensing matrix from spherical harmonics. We can formulate the problem as follows:

$$\underset{\theta_p,\phi_p,p\in[m]}{\text{minimize}} \quad \mu(\mathbf{A}) \quad \text{subject to} \quad \theta_p \in [0,\pi],\ \phi_p \in [0,2\pi) \tag{15}$$

These problems are non-convex in general since the Legendre polynomials and trigonometric polynomials $e^{j(k^{(r)}-k^{(q)})\phi_p}$ are non-convex. Therefore, the objective function contains many local maxima and minima. Furthermore, the problem becomes more complicated if we consider certain constraints on sampling patterns over the sphere. Indeed one can see that certain sampling patterns lead to maximum coherence due to symmetry property of spherical harmonics. This is demonstrated in the following theorem.

Theorem 3. *Let the matrix $\mathbf{A} \in \mathbb{C}^{m\times N}$ be constructed from samples of spherical harmonics $\mathrm{Y}_l^k(\theta,\phi)$ for a signal with bandwidth B using a sampling pattern that satisfies*

$$2k\phi_i \equiv 2k\phi_j \mod 2\pi, \forall i,j \in [m]$$

for some $-(B-1) \le k \le B-1$. Then the mutual coherence of this matrix attains its maximum, i.e., $\mu(\mathbf{A}) = 1$.

Proof. What is essential for the proof is the symmetry property of associated Legendre polynomials [25],[26, Eq. 47] stated as follows

$$P_l^{-k}(\cos\theta) = (-1)^k C_{lk} P_l^k(\cos\theta) \tag{16}$$

where $C_{lk} = \frac{(l-k)!}{(l+k)!}$. For the case of spherical harmonics, this implies that

$$\mathrm{Y}_l^{-k}(\theta,\phi) = (-1)^k \overline{\mathrm{Y}_l^k(\theta,\phi)} = (-1)^k \mathrm{Y}_l^k(\theta,\phi) e^{-j2k\phi}.$$

Now if $2k\phi_i \equiv 2k\phi_j \mod 2\pi$ for all $i,j \in [m]$, then $e^{-j2k\phi_i} = e^{-j2k\phi_j}$, and hence:

$$\mathrm{Y}_l^{-k}(\boldsymbol{\theta},\boldsymbol{\phi}) = C_k \mathrm{Y}_l^k(\boldsymbol{\theta},\boldsymbol{\phi})$$

for some constant C_k. This means that there are two columns of the matrix, corresponding to these two basis functions, totally coherent with each other and therefore yielding the coherence equal to one. □

Remark 4. The previous theorem precludes some familiar sampling patterns. For example, if the number of samples are odd and smaller than $2B-1$ for the equiangular sampling pattern on azimuth, $\phi_p = \frac{2\pi(p-1)}{m-1}$ for $p \in [m]$, then one will get a matrix of full coherence with columns corresponding to $k = \frac{m-1}{2}$ being totally coherent.

Finding the optimal sequence on $\theta_p, \phi_p,\ p \in [m]$ is difficult since we have two independent variables in a non-convex function. As it can be seen from the above theorem, the coherence is more sensitive to choice of ϕ_p. In this article, instead of looking for both $\theta_p, \phi_p,\ p \in [m]$, the choice of $\phi_p,\ p \in [m]$ is optimized given a fixed pattern on $\theta_p,\ p \in [m]$, for example, the class of equispaced and symmetric samples namely $\theta_p = \arccos(\frac{2p-m-1}{m-1})$, $p \in [m]$. This class of sampling patterns is easy to implement since it gives equispace property on the interval $[-1,1]$. The following theorem provides a lower bound on the coherence of this specific matrix.

Theorem 5 (Lower bound of a coherence of a matrix from spherical harmonics)**.** *For symmetric and equispaced sampling patterns with* $\cos\theta_p = \frac{2p-m-1}{m-1}, p \in [m]$*, the coherence of corresponding sensing matrix from spherical harmonics is lower bounded by*

$$\mu(\mathrm{A}) \geq \left| \sum_{p=1}^{m} \hat{P}_{B-1}(\cos\theta_p)\hat{P}_{B-3}(\cos\theta_p) \right| \tag{17}$$

where $\hat{P}_l(\cos\theta)$ *is the Legendre polynomial of degree* $l \in \{0,\dots,B-1\}$ *which is normalized with its* ℓ_2*-norm.*

Proof. Let us first write the coherence of a matrix which is sampled from spherical harmonics and write the lower bound as follows:

$$\begin{aligned}
\mu(\mathrm{A}) &= \max_{q\neq r} \left| \sum_{p=1}^{m} \frac{\mathrm{Y}_{l^{(q)}}^{k^{(q)}}(\theta_p,\phi_p)\overline{\mathrm{Y}_{l^{(r)}}^{k^{(r)}}(\theta_p,\phi_p)}}{\|\mathrm{Y}_{l^{(q)}}^{k^{(q)}}(\theta,\phi)\|_2 \|\mathrm{Y}_{l^{(r)}}^{k^{(r)}}(\theta,\phi)\|_2} \right| \\
&\geq \max_{\substack{l^{(q)}\neq l^{(r)} \\ k^{(r)}=k^{(q)}}} \frac{\left| \sum_{p=1}^{m} P_{l^{(q)}}^{k^{(q)}}(\cos\theta_p) P_{l^{(r)}}^{k^{(r)}}(\cos\theta_p) \right|}{\|P_{l^{(q)}}^{k^{(q)}}(\cos\theta)\|_2 \|P_{l^{(r)}}^{k^{(r)}}(\cos\theta)\|_2} \\
&\geq \max_{\substack{l^{(q)}\neq l^{(r)} \\ k^{(r)}=k^{(q)}=0}} \frac{\left| \sum_{p=1}^{m} P_{l^{(q)}}(\cos\theta_p) P_{l^{(r)}}(\cos\theta_p) \right|}{\|P_{l^{(q)}}(\cos\theta)\|_2 \|P_{l^{(r)}}(\cos\theta)\|_2} \\
&\geq \left| \sum_{p=1}^{m} \hat{P}_{B-1}(\cos\theta_p)\hat{P}_{B-3}(\cos\theta_p) \right|.
\end{aligned} \tag{18}$$

Note that by choosing $k^{(r)} = k^{(q)} = 0$, the associated Legendre polynomials become Legendre polynomials. Moreover if $l^{(q)}$ and $l^{(r)}$ are not both even or odd simultaneously, the corresponding sum $\left|\sum_{p=1}^{m} P_{l^{(q)}}(\cos\theta_p) P_{l^{(r)}}(\cos\theta_p)\right|$ is zero. This is because the product of Legendre polynomials would be an odd function summed over points symmetric around the origin. Therefore the choice of two consecutive maximum degree $l_1 = B-2$ and $l_2 = B-1$ leads to zero and instead $l_1 = B-3$ and $l_2 = B-1$ are chosen. □

Using a more demanding and complex proof, it can be shown that the last inequality in (18) is an equality if the number of measurements m are large enough. The proof is lengthy and is not presented here. It utilizes the following characterization of Legendre polynomials assuming $l_2 > l_1$:

$$P_{l_1}(\cos\theta_p) P_{l_2}(\cos\theta_p) = \sum_{\hat{l}=l_2-l_1}^{l_2+l_1} \eta_{\hat{l}}(l_1,l_2) P_{\hat{l}}(\cos\theta_p) \tag{19}$$

where $\eta_{\hat{l}}(l_1,l_2) = (2\hat{l}+1)\begin{pmatrix} l_1 & l_2 & \hat{l} \\ 0 & 0 & 0 \end{pmatrix}^2$ and $\begin{pmatrix} l_1 & l_2 & \hat{l} \\ 0 & 0 & 0 \end{pmatrix}$ is Wigner 3j-symbols. In this way, the inner products are represented as a linear combination of $P_{\hat{l}}(\cos\theta_p)$. For this choice of θ_p and regardless of the design for ϕ_p, the mutual coherence is absolutely lower bounded by choosing $l_1 = B-3$ and $l_2 = B-1$ which leads to a good lower bound as shown in the next section. In other words, the lower bound acts as a benchmark to see if ϕ_p's are chosen properly. The azimuth angle ϕ_p affects the coherence only through the exponential functions $e^{jk\phi_p}$. The goal is to choose those ϕ_p so that the maximum inner product is minimized. We will discuss a numerical approach to this problem in the next section.

4. NUMERICAL EXAMPLE

In this section, we will compare the coherence of sensing matrices from bandlimited spherical harmonics with $B = 7$ that are sampled by several well known sampling patterns on the sphere, for example spiral [27], Hammersley [28], Fibonacci [29], equiangular sampling, and our proposed sampling pattern with equispaced property on $\cos\theta$. In this numerical experiment, two equispaced samples on $\cos\theta$ will be used, namely $\cos\theta_p = \frac{2p-m-1}{m-1}$, $p \in [m]$ which is defined as sampling 1 and $\cos\theta_p = \frac{2p}{m}$, $p \in [-\frac{m-1}{2},\dots,\frac{m-1}{2}]$ as sampling 2, where m is odd for all sampling patterns. The pattern search algorithm [30] is used to find the vector $\boldsymbol{\phi} \in \mathbb{R}^m$ in (15) given the vector $\boldsymbol{\theta} \in \mathbb{R}^m$. The method is described in Algorithm 1. The

Algorithm 1 Pattern search

Initialization : $\boldsymbol{\theta}, \boldsymbol{\phi}_0 \in \mathbb{R}^m$ as initial points, $\Delta_0 > 0$ as initial step size, standard basis $\boldsymbol{e}_i$ for $i \in [m]$, $\lambda \in (0,1)$
for $k = 0, 1, \dots$ until *halting criterion* **do**
  if $\mu(\boldsymbol{\theta}, \boldsymbol{x}) < \mu(\boldsymbol{\theta}, \boldsymbol{\phi}_k)$ for $\boldsymbol{x} \in S_k := \{\boldsymbol{\phi}_k \pm \Delta_k \boldsymbol{e}_i\}$ **then**
    $\boldsymbol{\phi}_{k+1} = \boldsymbol{x} \mod 2\pi$
    $\Delta_{k+1} = \Delta_k$
  else
    $\boldsymbol{\phi}_{k+1} = \boldsymbol{\phi}_k \mod 2\pi$
    $\Delta_{k+1} = \lambda\Delta_k$
  end if
end for

algorithm starts by choosing uniformly random sampling on the interval $\phi \in [0, 2\pi)$. Pattern search method tries to find the minimum coherence and its minimizer by checking the neighboring vectors where the step size is given as Δ for every iteration. If the search is failed, then the step size is decreased by scaling with λ. The algorithm stops when the number of iteration is achieved or when the difference between the solution coherence and lower bound from the product of Legendre polynomials is small $|\mu^k - \mu_{LB}| \le \epsilon$. In general, this algorithm is heuristic and there is no guarantee that the solution will converge to the global optimum even though there is a discussion on the convergence of this algorithm, for example in [30]. However, as it can be seen numerically from Fig.1, the algorithm 1 could find a sequence $\phi_p \in [0, 2\pi)\,, p \in [m]$ achieving the Legendre bound of sampling 1 as discussed in Theorem 5. Hence, it shows the tightness of the Legendre bound for $l_1 = B - 3$ and $l_2 = B - 1$.

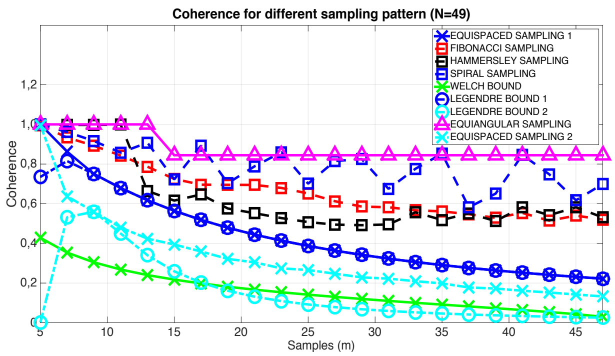

Fig. 1. Coherence of different sampling pattern

By using sampling 2, the coherence could be improved in general. However the lower bound becomes loose as it moves below the Welch bound, as numerically shown in Fig.1. Nevertheless, the lower bound is achieved for the number of sample $m = 9$. This construction avoids placing sampling points on the poles since the maximum of Legendre polynomials occurs on the poles ($\theta = \pi$ and $\theta = 0$). By avoiding these points, the coherence of the sensing matrix can be reduced. Furthermore, it shows that well known sampling patterns on the sphere, i.e spiral, Fibonacci and Hammersley points, do not tend to have lower coherence when the number of samples are increased. Therefore, those sampling patterns are not suitable to be used for designing sensing matrices. Additionally, the equiangular sampling gives the worst results as discussed in Remark 4.

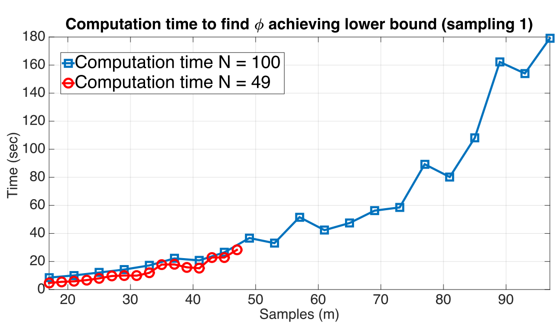

Fig. 2. Computation time of algorithm 1 for sampling 1

It is interesting to observe the computation time of the algorithm 1 in order to find azimuth angle $\boldsymbol{\phi} \in \mathbb{R}^m$ that could achieve the Legendre bound. In order to address this question, the computation time of Algorithm 1 for sampling 1 is given in Fig.2. In this figure, the numerical experiments for $N = 49$ and $N = 100$ are investigated with an error tolerance of $|\mu^k - \mu_{LB}| \le \epsilon = 10^{-4}$. When we double the dimension of the signal, it is apparent that the computation time to achieve the same error tolerance would increase approximately five-fold. However, as already discussed for sampling 2, it is difficult to achieve the Legendre bound and its computation time is longer than that of sampling 1.

4.1. Sparse recovery performance

In this section, the sensing matrices constructed from several sampling patterns are examined to recover sparse signal. The l_1-norm minimization package YALL1[31] is used to evaluate the phase transition diagrams with 50 trials, bandlimited degree $B = 7$ and $N = B^2 = 49$. Figure 3 presents the phase transition diagram of all sampling patterns. It can be seen that our proposed sampling pattern, namely equispaced and symmetric on the elevation gives better recovery performance compared to other sampling patterns. In contrast, equiangular sampling has the worst performance in terms of sparse recovery due to the coherence properties as discussed in Theorem 3.

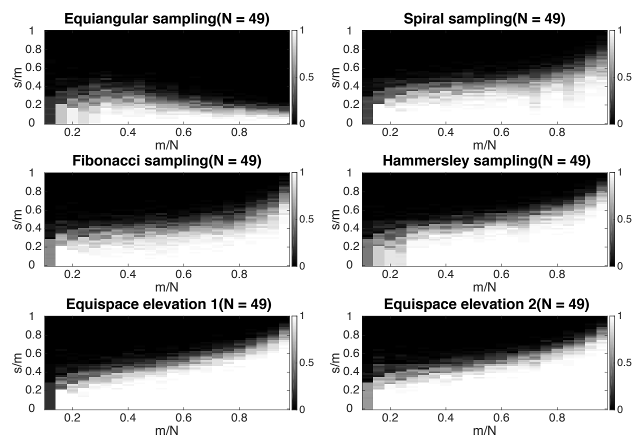

Fig. 3. Phase transition of different sampling pattern

5. CONCLUSION AND FUTURE WORKS

In this work, the coherence-based analysis of sensing matrices from spherical harmonics is discussed. It is shown in Theorem 3 that the equiangular sampling is not suitable to design a sensing matrix for sparse recovery. Using equispaced sampling pattern on $\cos\theta$, the lower bound of coherence could be obtained, which consists of the product two Legendre polynomials of different degrees. The degree should be chosen in such a way that the product of the Legendre polynomials is an even function. Numerically, for equispaced sampling on $\cos\theta$, it is possible to find a vector of azimuth angles $\boldsymbol{\phi} \in \mathbb{R}^m$ that could achieve the lower bound. This can be accomplished by implementing a simple pattern search algorithm. In future works, the framework will be extended to Wigner-D basis expansions and the theoretical background for the choice on ϕ will be addressed.

6. REFERENCES

[1] Afonso S Bandeira, Edgar Dobriban, Dustin G Mixon, and William F Sawin, "Certifying the restricted isometry property is hard," *IEEE Transactions on Information Theory*, vol. 59, no. 6, pp. 3448–3450, 2013.

[2] Andreas M Tillmann and Marc E Pfetsch, "The computational complexity of the restricted isometry property, the nullspace property, and related concepts in compressed sensing," *IEEE Transactions on Information Theory*, vol. 60, no. 2, pp. 1248–1259, 2014.

[3] A. Mazumdar and A. Barg, "General constructions of deterministic (Statistical) RIP matrices for compressive sampling," in *2011 IEEE International Symposium on Information Theory Proceedings*, July 2011, pp. 678–682.

[4] Philippe Delsarte, Jean-Marie Goethals, and Johan Jacob Seidel, "Spherical codes and designs," *Geometriae Dedicata*, vol. 6, no. 3, pp. 363–388, 1977.

[5] Henning Zörlein and Martin Bossert, "Coherence optimization and best complex antipodal spherical codes," *IEEE Transactions on Signal Processing*, vol. 63, no. 24, pp. 6606–6615, 2015.

[6] Thomas Strohmer and Robert W Heath, "Grassmannian frames with applications to coding and communication," *Applied and computational harmonic analysis*, vol. 14, no. 3, pp. 257–275, 2003.

[7] David J Love, Robert W Heath, and Thomas Strohmer, "Grassmannian beamforming for multiple-input multiple-output wireless systems," *IEEE Transactions on Information Theory*, vol. 49, no. 10, pp. 2735–2747, 2003.

[8] Yonina C Eldar and G David Forney, "Optimal tight frames and quantum measurement," *IEEE Transactions on Information Theory*, vol. 48, no. 3, pp. 599–610, 2002.

[9] Andrew J Scott, "Tight informationally complete quantum measurements," *Journal of Physics A: Mathematical and General*, vol. 39, no. 43, pp. 13507, 2006.

[10] Petros Drineas, Malik Magdon-Ismail, Michael W Mahoney, and David P Woodruff, "Fast approximation of matrix coherence and statistical leverage," *Journal of Machine Learning Research*, vol. 13, no. Dec, pp. 3475–3506, 2012.

[11] Mehryar Mohri and Ameet Talwalkar, "Can matrix coherence be efficiently and accurately estimated?," in *Proceedings of the Fourteenth International Conference on Artificial Intelligence and Statistics*, 2011, pp. 534–542.

[12] Michael Elad, "Optimized projections for compressed sensing," *IEEE Transactions on Signal Processing*, vol. 55, no. 12, pp. 5695–5702, 2007.

[13] Cristian Rusu and Nuria González-Prelcic, "Designing incoherent frames through convex techniques for optimized compressed sensing," *IEEE Transactions on Signal Processing*, vol. 64, no. 9, pp. 2334–2344, 2016.

[14] Simon Foucart and Holger Rauhut, *A mathematical introduction to compressive sensing*, Springer, 2013.

[15] Lloyd Welch, "Lower bounds on the maximum cross correlation of signals (corresp.)," *IEEE Transactions on Information Theory*, vol. 20, no. 3, pp. 397–399, 1974.

[16] Matthew Fickus and Dustin G Mixon, "Tables of the existence of equiangular tight frames," *arXiv preprint arXiv:1504.00253*, 2015.

[17] Jesper E Hansen, *Spherical near-field antenna measurements*, vol. 26, IET, 1988.

[18] Erwan Thébault, Christopher C Finlay, Ciarán D Beggan, Patrick Alken, Julien Aubert, Olivier Barrois, Francois Bertrand, Tatiana Bondar, Axel Boness, Laura Brocco, et al., "International geomagnetic reference field: the 12th generation," *Earth, Planets and Space*, vol. 67, no. 1, pp. 79, 2015.

[19] Boaz Rafaely, "Analysis and design of spherical microphone arrays," *IEEE Transactions on speech and audio processing*, vol. 13, no. 1, pp. 135–143, 2005.

[20] Holger Rauhut and Rachel Ward, "Sparse recovery for spherical harmonic expansions," *arXiv preprint arXiv:1102.4097*, 2011.

[21] Nicolas Burq, Semyon Dyatlov, Rachel Ward, and Maciej Zworski, "Weighted eigenfunction estimates with applications to compressed sensing," *SIAM Journal on Mathematical Analysis*, vol. 44, no. 5, pp. 3481–3501, 2012.

[22] Rasmus Cornelius, Arya Adiprakasa Bangun, and Dirk Heberling, "Investigation of different matrix solver for spherical near-field to far-field transformation," in *Antennas and Propagation (EuCAP), 2015 9th European Conference on*. IEEE, 2015, pp. 1–4.

[23] R Cornelius, D Heberling, N Koep, A Behboodi, and R Mathar, "Compressed sensing applied to spherical near-field to far-field transformation," in *Antennas and Propagation (EuCAP), 2016 10th European Conference on*. IEEE, 2016, pp. 1–4.

[24] Benjamin Fuchs, Laurent Le Coq, Sébastien Rondineau, and Marco Donald Migliore, "Fast antenna far-field characterization via sparse spherical harmonic expansion," *IEEE Transactions on Antennas and Propagation*, vol. 65, no. 10, pp. 5503–5510, 2017.

[25] Izrail Solomonovich Gradshteyn and Iosif Moiseevich Ryzhik, *Table of integrals, series, and products*, Academic press, 2014.

[26] G Lohöfer, "Inequalities for the associated Legendre functions," *Journal of Approximation Theory*, vol. 95, no. 2, pp. 178–193, 1998.

[27] Edward B Saff and A BJ Kuijlaars, "Distributing many points on a sphere," *The mathematical intelligencer*, vol. 19, no. 1, pp. 5–11, 1997.

[28] Jianjun Cui and Willi Freeden, "Equidistribution on the sphere," *SIAM Journal on Scientific Computing*, vol. 18, no. 2, pp. 595–609, 1997.

[29] Richard Swinbank and R James Purser, "Fibonacci grids: A novel approach to global modelling," *Quarterly Journal of the Royal Meteorological Society*, vol. 132, no. 619, pp. 1769–1793, 2006.

[30] Virginia Torczon, "On the convergence of pattern search algorithms," *SIAM Journal on optimization*, vol. 7, no. 1, pp. 1–25, 1997.

[31] Y Zhang, J Yang, and Wotao Yin, "YALL1: Your algorithms for L1," *MATLAB software, http://www. caam. rice. edu/˜ optimization L1*, vol. 1, 2010.